

Impact Assessment of Agro-Meteorological Drought Using Geo-Spatial Techniques. A Case Study of Southeastern Sindh-Pakistan

Saira Batool¹, Syed Amer Mahmood², Jahanzeb Qureshi², Amer Masood², Maryam Muhammad Ali², Zainab Tahir²

¹Centre for Integrated Mountain Research

²Department of Space Science, University of Punjab Lahore

*Correspondence: sairabnaqvi5@gmail.com

Citation | Batool. S, Mahmood. S. A, Qureshi. J, Masood. A, Ali. M. M, Tahir. Z, "Impact Assessment of Agro-Meteorological Drought Using Geo-Spatial Techniques. A Case Study of Southeastern Sindh-Pakistan", IJIST, Special Issue pp 455-471, June 2024

Received | June 11, 2024 **Revised** | June 16, 2024 **Accepted** | June 20, 2024 **Published** | June 28, 2024.

The frequency of droughts is rising as the global temperature rises significantly. Therefore, it's essential to utilize the right index when monitoring drought conditions. SPI and RDI tools were utilized in this study to evaluate the drought situation. "DrinC" was used to generate the Reconnaissance Drought Index (RDI) for the 3-, 6-, and 12-month (Oct-Dec, Oct-March, and Oct-September) time periods from 1981 to 2020. With RDIs between -1.0 and -2.5, all districts experience moderate, severe, and extreme droughts. The RDI 3-, 6-, and 12-month Calculations were used to emphasize the years 1984, 1992, 1994, 2010, 2011, 2015, and 2019. These findings demonstrate that in years of drought, productivity decreased. Most stations experienced dry weather between 1981 and 2020. In South-Eastern Sindh, Pakistan, during the past four decades (1981-2020), this study intends to assess changes in land surface temperature (LST), Normalized Difference Vegetation Index (NDVI), and Soil Moisture Index (SMI). LST changes were analyzed using approaches for identifying satellite data. The highest NDVI reading was obtained in 1988 (+0.53), and the lowest reading was obtained in 2021 (+0.48). The greatest SMI was found to be (+1.1) in 1988, while the minimum was found to be (+0.98) in 2021. Similarly, the LST ranged from 35.1 degrees Celsius in 1988 to 53.4 degrees Celsius in 2021. SPI and RDI had a negative connection, according to the linear regression. For assessing the severity of drought conditions, the SPI and RDI indexes are useful. The results suggested that these techniques might be helpful in creating drought preparedness plans. Such research could be beneficial for the creation of tactical approaches to fend against droughts and decrease their effects on various economic sectors.

Keywords: Climate change, RDI, SPI, Remote sensing, NDVI, LST, SMI, Geospatial techniques



Introduction:

Described as a lengthy period of below-average natural water availability that takes place on a regional scale, drought is a natural occurrence that can occur everywhere in the world [1][2]. As a result of global warming brought on by a rise in greenhouse gases, droughts are anticipated to occur more frequently. Water demand and availability are projected to fluctuate spatially and over time as a result of global warming [3]. Drought is a severe natural calamity that affects a variety of economic sectors and has a terrible effect on the lives of the poor globally. Most scientists agree that there are several causes of drought. Depending on who you ask, drought is defined differently; for example, agriculturists link it to a lack of moisture (also known as "effective precipitation" [4], which has a negative impact on crop yields; meteorologists, meanwhile, define it as a persistent lack of rainfall; and hydrologists, with decreased water run-off. Climate change is the primary driver of drought, and these changes emphasize the relative importance of evapotranspiration (ET), rainfall, and water run-off [5]. Numerous people and broad regions are impacted by frequent, complex, and global droughts [6].

According to climate change predictions, an increase in average global temperatures will have an impact on evapotranspiration and specific air moisture, which will affect the amount of water that can be stored in the atmosphere and have a direct impact on rainfall's size, duration, intensity, and geospatial dispersion [7]. Meteorological drought, which includes the weather and climatic processes and reduces surface and groundwater levels, decreases water supply, and degrades water quality, can result in hydrological drought. The cyclical pattern of drought in Africa over many years has had various negative effects, including mortality, crop failures, and food scarcity [8]. According to researcher [9], these have induced malnutrition in a number of locations, which has resulted in hunger, sickness, and population relocation. Between 1900 and 2010, drought directly caused over ten million deaths. In Europe, droughts in 2003 and 2006 reduced agricultural output, complicated navigation, and resulted in fatalities. The last drought, which didn't end until 2008, had a long-lasting impact on the Mediterranean region by reducing groundwater resources and storage conditions.

Even if the event continues towards rising precipitation and temperatures with a greater likelihood, droughts may be a problem [10]. These may have a significant impact on Pakistan's agro-climatic regions, especially in the arid regions. Sindh and Baluchistan may experience two to three water crises yearly and are more susceptible to drought than Punjab, Khyber Pakhtunkhwa, and Baluchistan. The crop moisture index, the vegetation condition index (VCI), the temperature condition index (TCI), the deciles index, and the standard water-level index (SWI) are a few of the roughly 15 indicators that are frequently used [11]. These indices use big data sets to estimate drought in slightly different ways. The standard precipitation indicator (SPI) is widely used in drought research in the region [12]. The World Meteorological Organization (WMO) advises using the reconnaissance drought index (RDI) and standard precipitation index (SPI) to characterize droughts [13]. Through the use of several metrics, drought can be visualized on various time scales. The reconnaissance drought index was selected for this study since it was developed to account for water scarcity and characterize drought by combining temperature and precipitation data [14]. Research at a small spatial scale benefits most from RDI, while studies at different time scales benefit most by SPI analysis.

Before it suddenly bursts out in a few years, the population may be unaware of the drought for a few years. People only become aware of it after the effects of the drought have already started [15]. Droughts have become more frequent in Sindh as a result of changed weather patterns and pollution levels. In order to help disaster mitigation managers and other stakeholders put the current drought in historical perspective, this study looks at the previous variations of droughts in the Pakistani districts of Sindh.

Material and Methods:

Study Area:

The Sindh province of Pakistan is situated in the southeast of the nation. It includes a total of 23 districts and lies between the latitudes of 25.8943° N and 68.5247° E, making up around 18% of the nation's total land area (140,914 km²). It shares borders with the Pakistani provinces of Baluchistan to the north and Punjab to the northeast as well as the Indian states of Rajasthan and Gujrat to the east. With maximum temperatures ranging from 27.08° C in the winter to 43.32° C in the dry summer, Sindh experiences an average yearly precipitation of 128.80 mm.

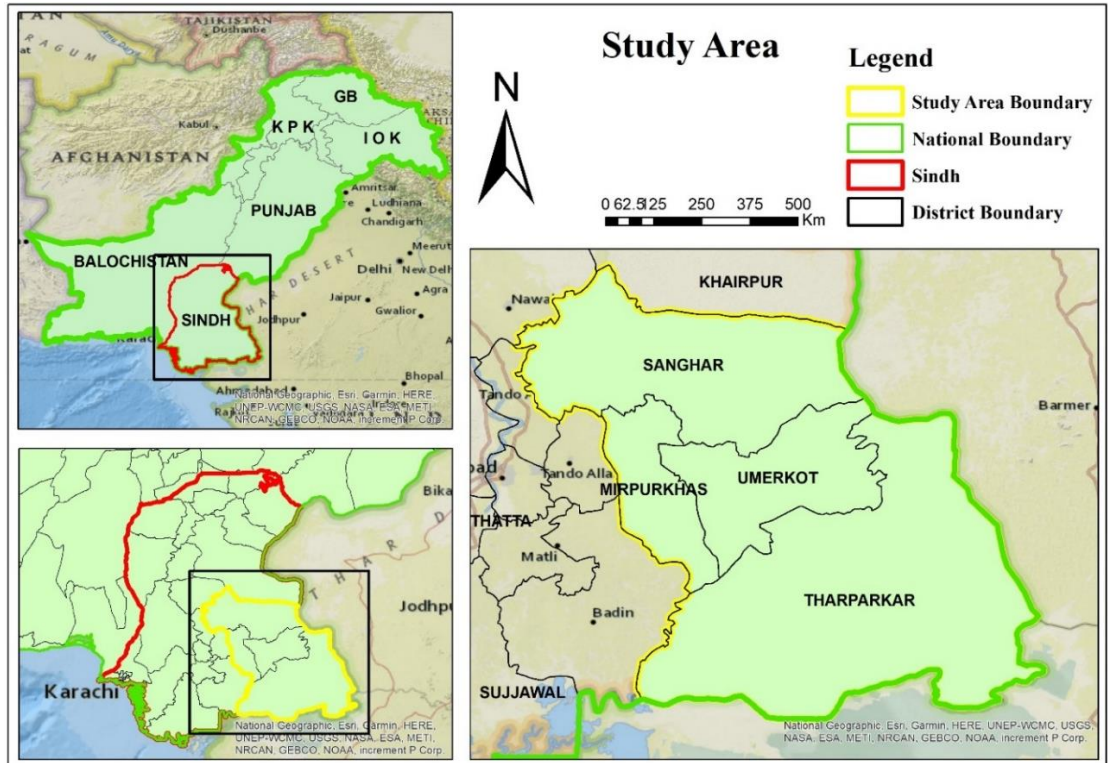


Figure 1: Map of Study Area

Data Acquisition:

Our research employed temperature and average precipitation data that were collected from the meteorological department for the years 1981 to 2020. It was determined the Standard Precipitation Index (SPI) and Reconnaissance Drought Index (RDI) indices. DrinC (Drought indices Calculator) makes it simple to compute the aforementioned indices for one year, six months, nine months, and three months using the gamma and log-normal approaches, respectively. There is a connection between the RDI and SPI. However, according to researcher [16], the RDI is calculated by fitting the gamma distribution to the yearly rainfall and PET data. For the geographical and temporal study of variables including temperatures, soils, and rainfall, geographic information system (GIS) approaches are essential for agricultural modelling [17]. GIS interpolation technologies were used to understand the spatial characteristics and frequency of droughts in the research area [18]. We employed the IDW approach of the Geospatial interpolated in this investigation. Researchers use data on vegetation and land surface temperature to calculate the soil moisture index. The USGS Earth Explorer website provided the Landsat 8 satellite pictures that were used in this investigation; the images have a spatial resolution of 30m. Red and near-infrared (NIR) bands are required for the NDVI estimation. Thermal infrared (TIR) bands are necessary for the land surface temperature (LST) computation [19].

Standardized Precipitation Index (SPI):

By estimating a probabilistic model to a geographic data set of rainfall amount, developed the SPI probability indicator for drought monitoring [20]. In order to distinguish dry

and wet seasons across various time periods in diverse locations of the world, a drought indicator was developed. SPI makes it possible to calculate the frequency of droughts over time for any location [17]. This index is recommended by the World Meteorological Organization (WMO) to calculate the amount of rainfall that fell over a certain time period. The average SPI for the region and time period of concern is zero thanks to the transformation of rainfall data into a widely distributed function [21].

X stands for precipitation during a certain time period, and stands for probability density. $f(x) = 1 / ((\sigma \sqrt{2\pi})) \times (-1) e^{-(x/\sigma)^2} \times > 0 \ 1$ where μ and σ are the parameters defining the form and scale of respectively. SPI readings that are positive or negative represent greater or lesser rainfall than the norm. High negative SPI readings point to a very dry condition.

Reconnaissance Drought Index (RDI):

For drought monitoring and assessment, Tsakiris and Vangelis developed the Reconnaissance Drought Index (RDI) in 2005 [17]. The foundation of RDI is the combination of total precipitation (P) and potential evapotranspiration (PET), for which P is observed and PET is estimated. Due of its efficiency, Hargreave's approach has been widely used in semi-arid and arid regions [22]. The initial value RDI (k), the normalized RDI (nor), and the standardized RDI (std) are three different ways the RDI may be used to assess and manage droughts. The values are entered into the equation to calculate the RDI (assuming the log-normal distribution is being utilized).

$$RDI_{std}(i) = y(i) - y / y \quad 2$$

According to researcher [23], $y(i)$ is the $\ln(ak(i))$, y is its arithmetic mean, and y is its standard deviation. In comparison to the average for the region, positive RDI indicates wetter conditions, while negative RDI indicates drier conditions. Drought intensity ranges from 2.0 (severe) to 1.0 (moderate).

Table 1: Classification of droughts according to SPI and RDI values [17]

RDI and SPI	Classes
≥ 2.00	Extremely wet
1.5 to 1.99	Severely wet
1.0 to 1.49	Moderately wet
0.0 to 0.99	Normal
0.0 to -0.99	Mild drought
-1.00 to -1.49	Moderate drought
-1.50 to -1.99	Severe drought
≤ -2.00	Extreme drought

Calculation of LST NDVI and Soil Moisture Index (SMI):

The formula for calculating the soil moisture index [24] uses a realistic description of the relationship between land surface temperature (LST) and normalized difference vegetation index (NDVI)

$$: SMI = (LST_{max} - LST) / (LST_{max} - LST_{min}) \quad 3$$

The highest and minimum surface temperatures for a given NDVI are known as LST max and LST min, respectively. LST stands for Land Surface Temperature. We can determine the surface temperature of pixels at a specific NDVI from satellite photos. By resolving Equations, the maximum and minimum LSTs can be calculated.:

$$LST_{max} = a1 * NDVI + b1 \quad 4$$

$$LST_{min} = a2 * NDVI + b2 \quad 5$$

While the cold and warm sides of the dataset are defined by (current slopes and (b current interception), and (a or b) are the real variables obtained from the regression analysis. Equation (1) is used to translate the digital number (DN) into the radiance (LW/m2/sr/m), which is the first step in calculating SMI.

$$L = LST_{min} + (((LST_{max} - LST_{min}) / (QCAL_{max} - QCAL_{min})) * (DN - QCAL_{min})) \quad 6$$

Maximum and minimum quantization calibrate the number of pixels, QCAL max, QCAL min, and the Digital Numbers where LST min and LST max are parameters used to measure spectral radiance. The maximum and minimum values of LST must be calculated by evaluating two inputs (NDVI and LST). Utilizing the Landsat 5 and Landsat 8 Thermal channels, the equation calculates LST(K).

$$LST = Tb / [1 + (\lambda * Tb / C2) * \ln(\epsilon)] \tag{7}$$

Where Tb is the illumination temperature of the satellites, λ is the wavelengths of the radiation emitted, C2 = 1.4388 * 10² m K, and ε is the emissivity. The normalized difference vegetation index (NDVI), which is obtained from satellite data, is a statistic used to assess plant health. Using a cutting-edge, high-resolution radiometer, scientists can tell if the flora is thriving or withering away and becoming rarer. This method can be used to track changes in temperature, land use, and types of flora. For use in risk analyses and locating places with insufficient water supply, it is possible to identify plant groups that are susceptible to drought.

$$NDVI \text{ (Landsat 8 OLI): } NIR=B5, R=B4 \tag{8}$$

$$NDVI \text{ (Landsat 5 TM): } NIR=B4, R=B3 \tag{9}$$

Table 2: NDVI values for different types of cover

NDVI Range	Type of Cover
NDVI ≤ 0	Bare soil or water
0 to 0.2	Sparsely Vegetation
0.2 to 0.4	Less vegetation
0.4 to 0.6	Moderate Vegetation
0.6 to 0.8	Dense vegetation
0.8 to 1	Thick greenery

Linear Regression Analysis:

The statistical method of linear regression examines the relationship between two variables. Through linear regression, the relationship between two variables is investigated. The statistical method used the most frequently is linear regression analysis. The typical rate of change over time for the variables of interest is displayed by parametric approaches like the LR (slope) [25]. The data set's trend increases if the average periodic change curve of the factors under consideration is positive, and vice versa for negative values [26]. The RDI and SPI can be used to assess meteorological droughts that last three, six, nine, or twelve months. In the Sindh region, there was a significant link between RDI and SPI.

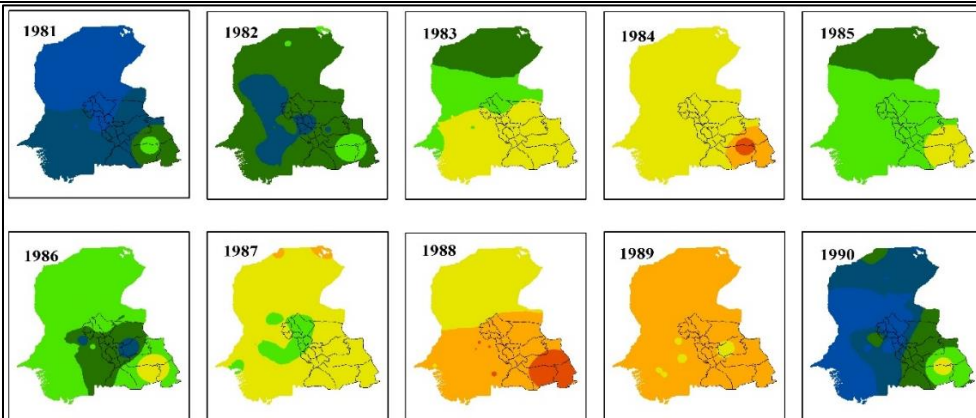
Results and Discussion:

Spatio Temporal Analysis of RDI:

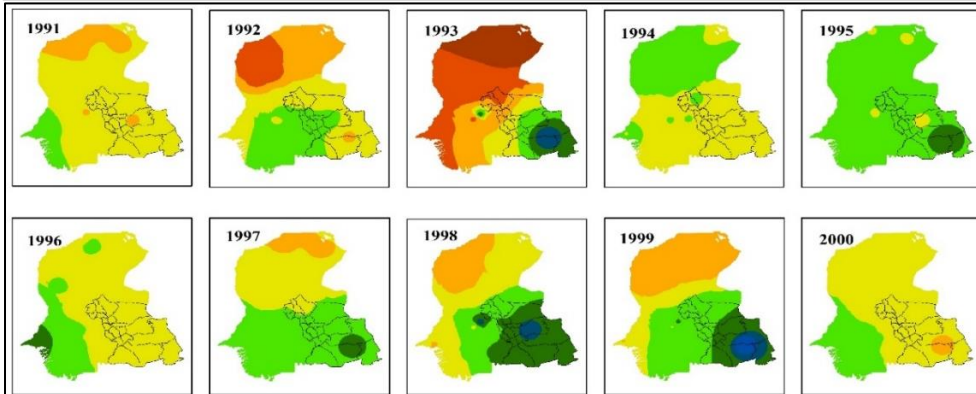
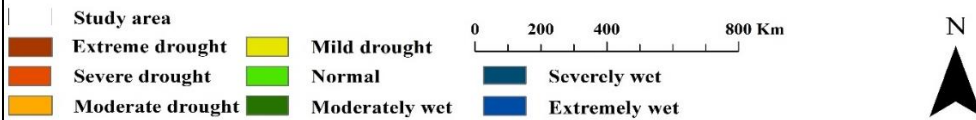
The three distinct RDI periods (3, 6, and 12 months) were combined using inverse distance weighting (IDW) interpolation to produce a geographical description of drought [27]. IDW data is trustworthy and does not entail autocorrelation because it is gathered for a specific area and time period [28]. The length of the drought is shown in images of geographic displays of RDI values created in Arc GIS 10.8 (Figure 9–11). The geospatial research assessed periods with RDI values. The interpolated images were produced using the only data that was available at the time.

Analysis of Three Months RDI Values:

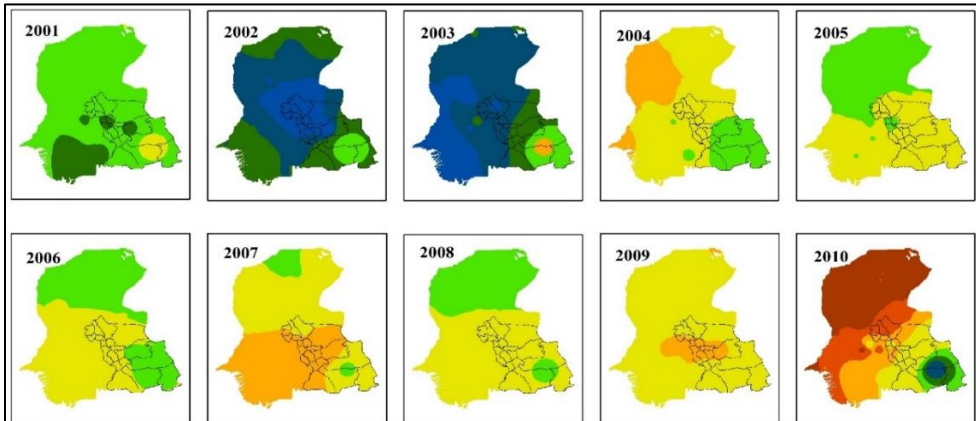
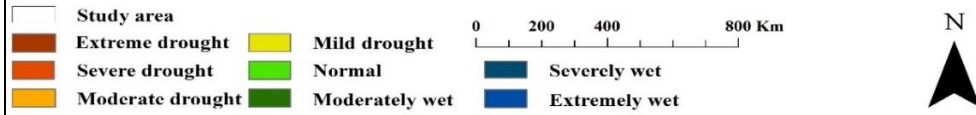
These findings show that the RDI values in the geographical areas that have been adversely affected by the drought differ noticeably from one another. According to data, Sindh only suffered extreme drought in 1993 and 2010 overall, not throughout the full study region. In the studied area, severe droughts spread widely in 1984, 1988, 1992, 2010, and 2011. In 1984, 1988, 1989, 1991, 1992, 1993, 2009, 2010, 2011, 2012, 2015, and 2019 there were numerous moderate droughts. Other years range from somewhat dry to extraordinarily wet circumstances. The Sindh region experienced above-average rainfall in 2013 and 2020.



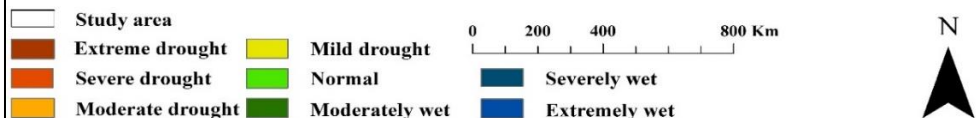
RDI-3 spatial-temporal patterns of drought



RDI-3 spatial-temporal patterns of drought



RDI-3 spatial-temporal patterns of drought



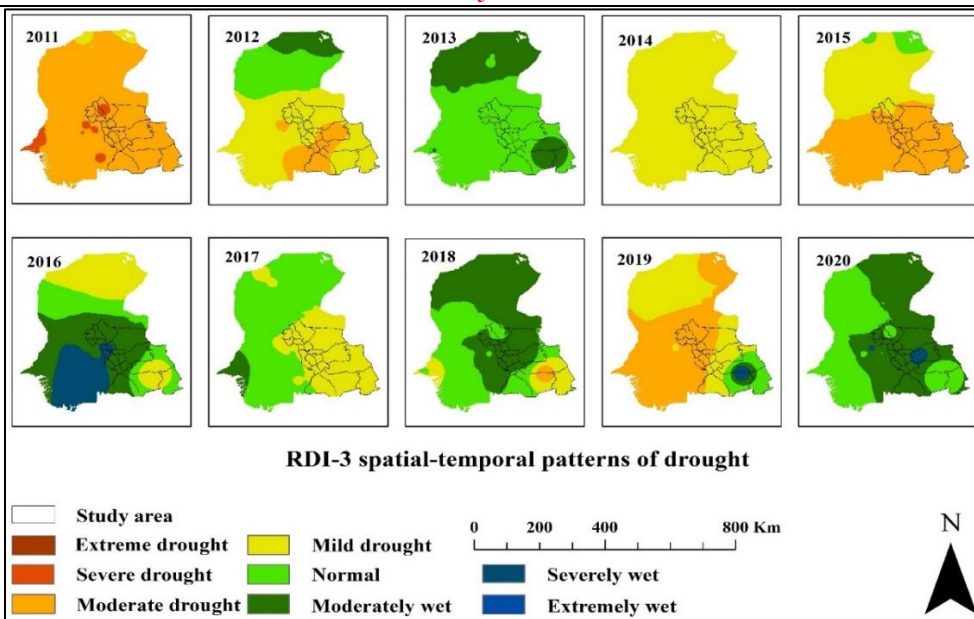
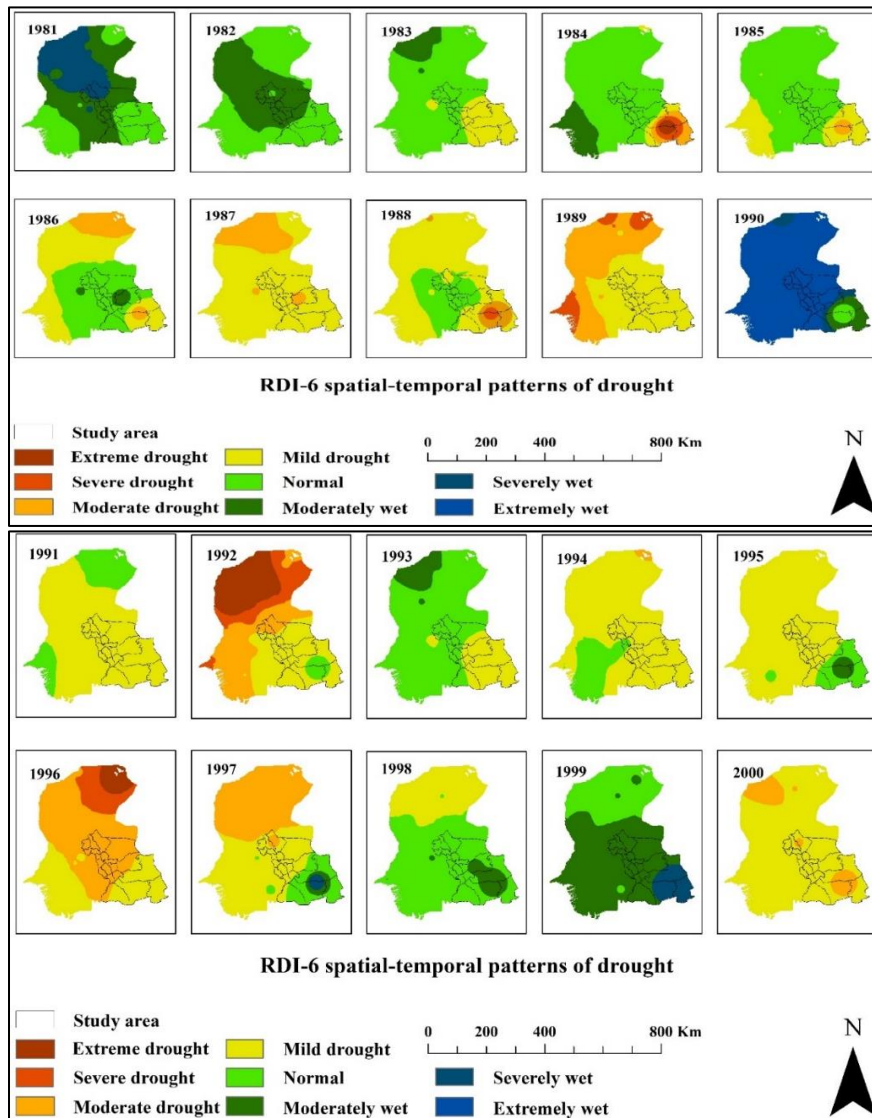


Figure 2: RDI-3 spatial-temporal patterns of drought for the years (1981–2020) based on RDI values



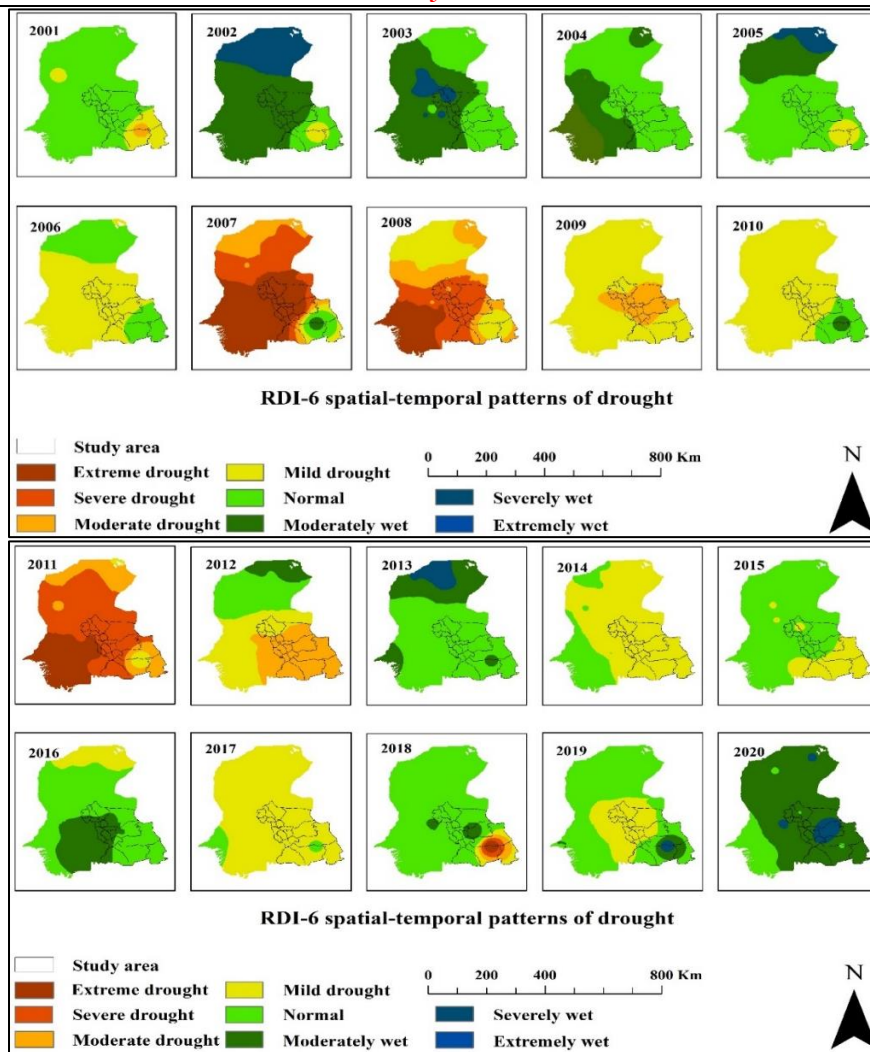


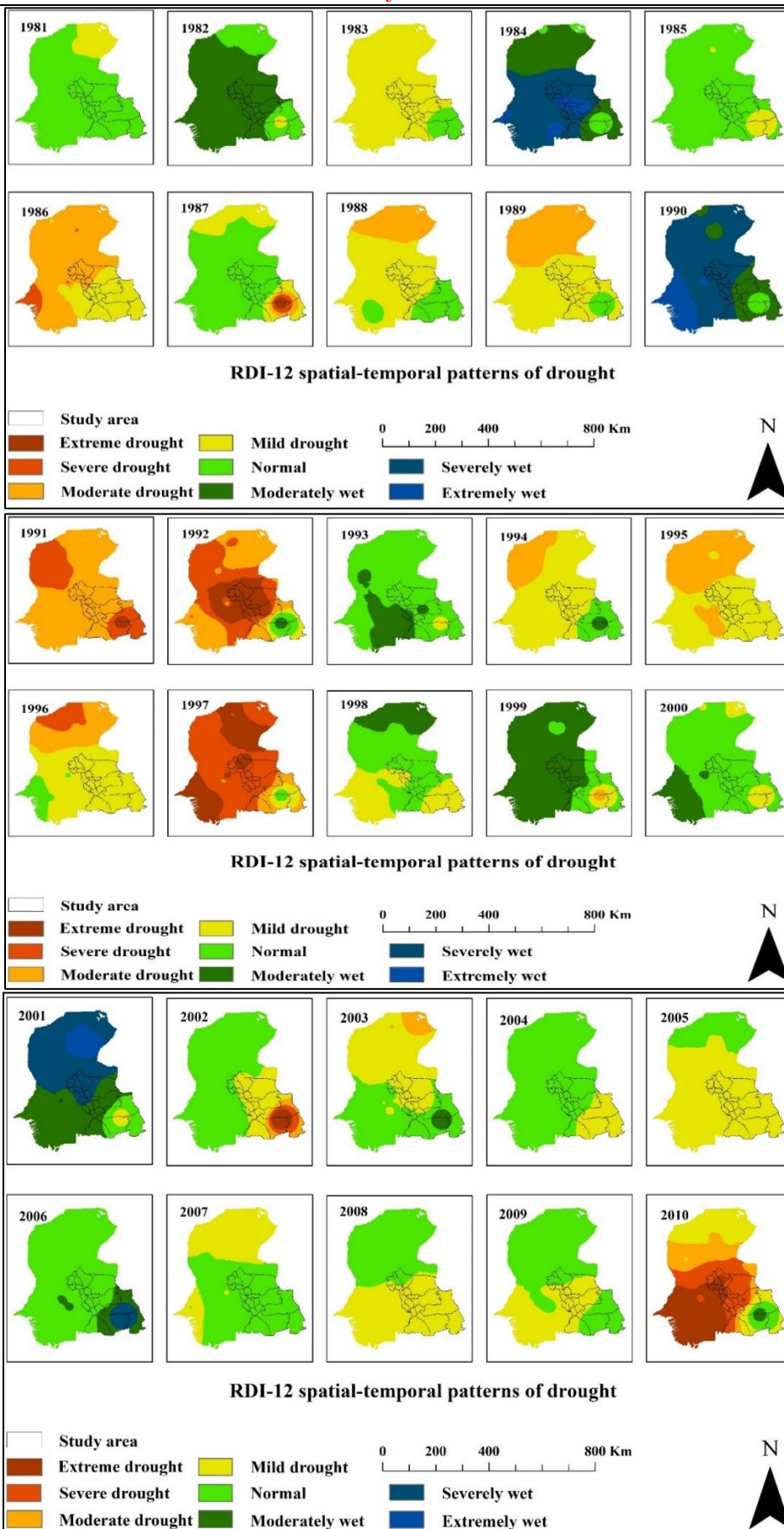
Figure 3: RDI-6 spatial-temporal patterns of drought for the years (1981–2020) based on RDI values

Analysis of Six Months RDI Values:

According to the regional analysis based on the RDI-6 results, there were widespread effects from mild to severe droughts in about 22 out of every 40 years. Extreme drought was reported in the study area in the years 2007, 1984, and 2011. Most of the cities have seen rainfall that is above average for the past 16 years, with the Sindh region being especially rainy every year. For the entirety of the study region, extremely rainy weather was noted in 1990.

Analysis of 12 Months' RDI Values:

According to the spatial analysis of the RDI-12 figures, the study area experienced widespread mild-to-extremely wet drought conditions for around 27 years. The years 1982, 1993, 1999, 2012, and 2015 saw above-average rainfall. Drought conditions that were extreme and severe were noted in 1987, 1991, 1992, 1997, 2002, 2010, and 2014. There were moderate drought occurrences in 1986, 1991, 1997, and 2014. All districts saw rainfall conditions that were above average in 1982 and 2015.



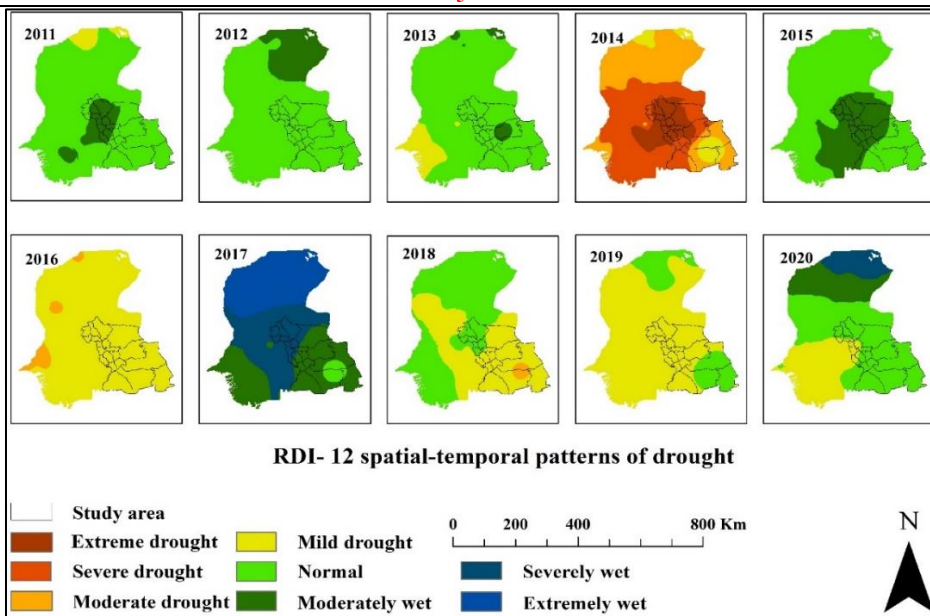


Figure 4: RDI-12 spatial-temporal patterns of drought for the years (1981–2020) based on RDI values

Correlation Between SPI and RDI:

The scatter graph of the SPI value versus RDI is shown in Figure 5-8. When the SPI and RDI data are plotted against one another, the differences between the two indices frequently grow larger with a longer time lag. On every time scale, there is a large uniformity between the two indices. Our research indicates that the two indicators we investigated for identifying droughts perform remarkably effectively.

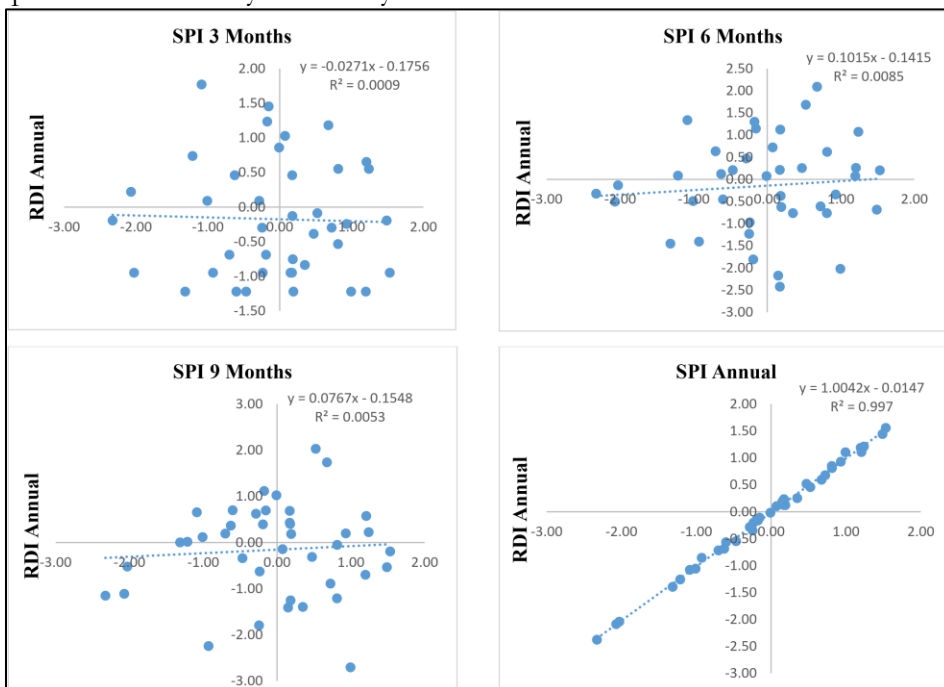


Figure 5: Comparison of SPI 3-, 6-, 9- and 12-months Vs. RDI Annual (Mirpurkhas)

The RDI and SPI can also be used to calculate the length of the drought over the next 3, 6, and 12 months. Due to the strong link between the RDI and SPI values in the Sindh region, Figure 5-8 illustrates the linear trend line derived across the various categories. The results demonstrated a significant relationship between the RDI and SPI. Even with just rainfall data, the graphs' algorithm allows one to calculate the RDI and precisely forecast drought-prone

seasons. In a linear regression study, the Yearly SPI and Yearly RDI fit quite closely, as indicated by an R2 of 0.998. The first three months of the SPI, the second three months of the SPI, the third and fourth months of the SPI, the first six months of the SPI, and the first nine months of the SPI were compared to the annual RDI values in the regression analysis. The best strategies are described in all of the illustrations. SPI values from the first nine months, half, and first quarter were used to calculate the annual RDI times, and the calculations were found to be robust with a high R2 value. These findings suggest that if the first three months of rainfall data are provided and the SPI is calculated for the following years, it is possible to forecast the RDI drought indices.

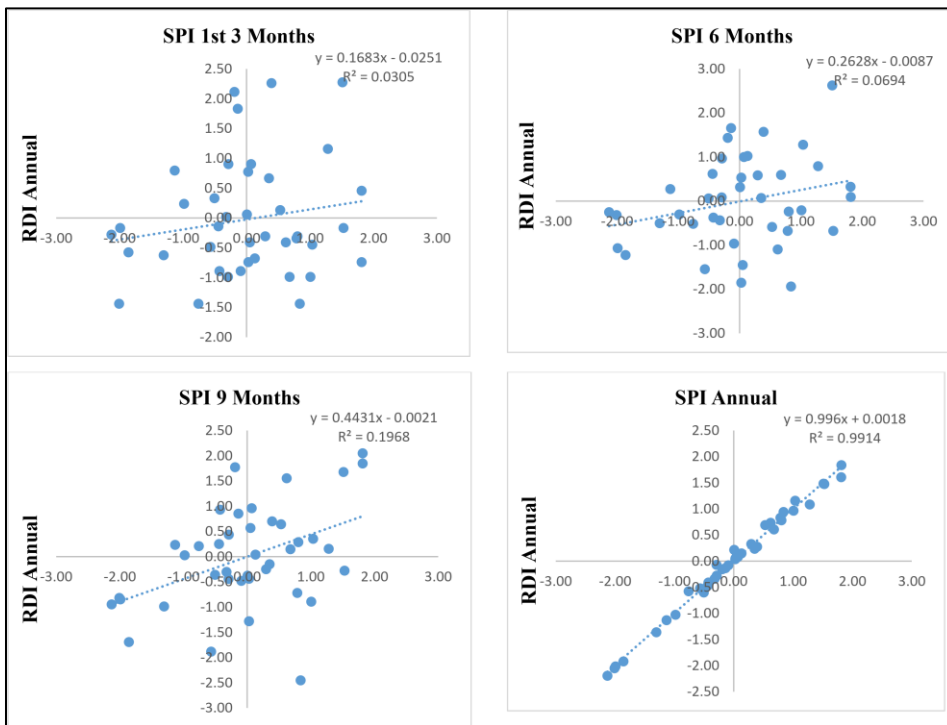


Figure 6: Comparison of SPI 3-, 6-, 9- and 12-months Vs. RDI Annual (Shanghar)

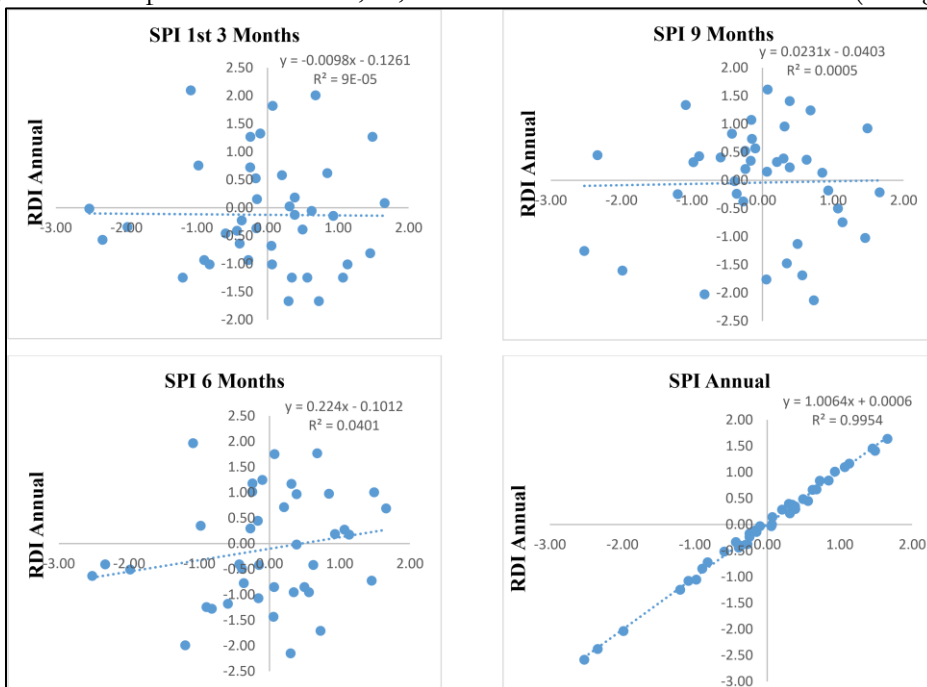


Figure 7: Comparison of SPI 3-, 6-, 9- and 12-months Vs. RDI Annual (Tharparkar)

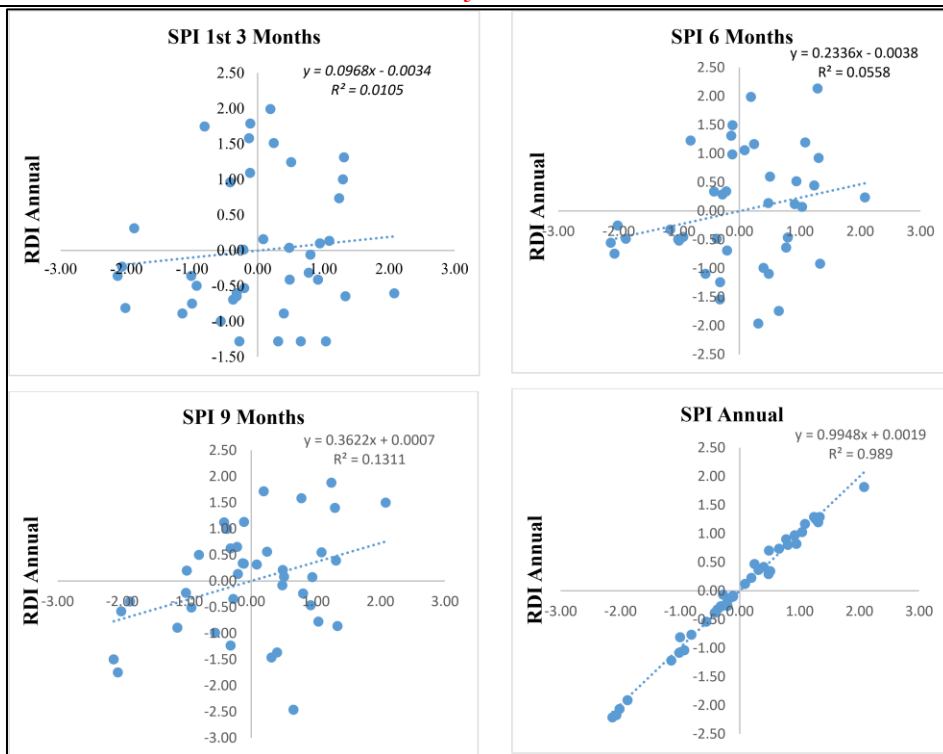


Figure 8: Comparison of SPI 3-, 6-, 9- and 12-months Vs. RDI Annual (Umerkot) **Normalized Difference Vegetation Index (NDVI) Changes:**

Through the use of Landsat pictures from 1988, 1998, 2008, 2018, and 2021, the NDVI model was created. The vegetation cover was identified using ArcGIS software. In the studied area, the NDVI values ranged from 0.99 to + 0.53 in 1988, 0.78 to + 0.81 in 1998, 0.99 to + 0.99 in 2008, and 0.75 to + 0.49 in 2018. However, in 2021, the NDVI values altered (minimum 0.2 and maximum +0.48). Greater NDVI values indicated the presence of the most productive terrain, such as vegetation and forests. On the other hand, locations with lower NDVI values, such as bare soil, waterbodies, and built-up areas, are less productive. As a result, the study region's most productive area displays a significant fall on the NDVI map. The NDVI value is generally higher in forest areas than it is for bare soil, so the study area's expanded vegetation area may have an impact on the vegetation's overall level of greenness as measured by satellite. It was observed that there was a significant (NDVI value) change between 1988 and 1998. The results demonstrate that the NDVI values in the chosen district rose over time.

Land Surface Temperature (LST) Changes:

Figure 9 shows the spatial pictures and areal distribution of LST in the districts of Shanghar, Umerkot, Tharparkar, and Mirpurkhas in five different years separated by a ten-year interval: 1988, 1998, 2008, 2018, and 2021. The variations in the research area are shown by the spatial patterns of LST. LST was generally predicted to be between 35.16 and 17.39°C in 1988, 53.8 to -69.40°C in 1998, 40.00 to 24.38°C in 2008, 47.54 to 25.4°C in 2018, and 53.44 to 25.77°C in 2021. Between 1988 and 2021, the research region's vegetation decreased and the build-up area increased, increasing the LST. Because of the greater amount of flora and agricultural land, namely Shanghar, the northern section of the research region has a lower temperature. In contrast, the center (Umerkot) shows an increase in LST as a result of accelerated urbanisation and declining water bodies and vegetative cover. The difference between estimated and recorded LST is acceptable when all the constraints of RS-derived LST estimation are taken into account, and it can be used for future analysis such as LST simulation and a temperature condition index in the study area. Additionally, according to Pakistan's agricultural calendar, September is a

month with a large amount of vegetation cover and when the research area's maximum LST values were assessed.

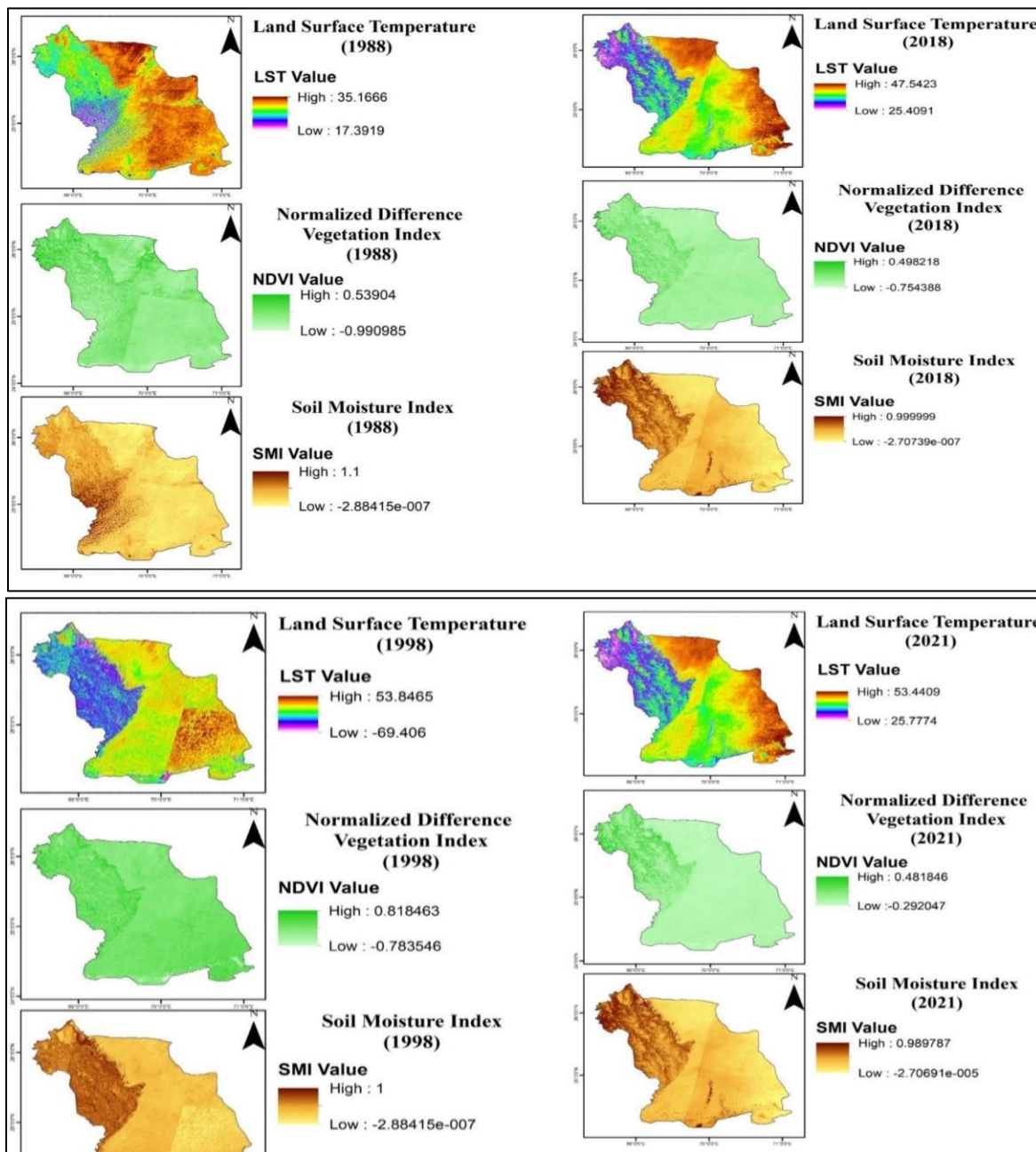


Figure 9: Spatio-temporal analysis of LST, NDVI and SMI in 1988, 1998, 2008, 2018 and 2021

Soil Moisture Index (SMI) Change:

The soil moisture index (SMI) displays a value between 0 and 1, where 0 represents the lowest SMI value and 1 represents the greatest SMI on a given date, reflecting the relative amount of soil moisture in the area. It is not possible to do a quantitative comparison between several days there for the month of September chosen here before calibration of the soil moisture indices measurements. The graph demonstrates that the moisture level was high enough in 1988 and later; however, after the year 2018, it declined to 0.99 and then 0.98 after three years.

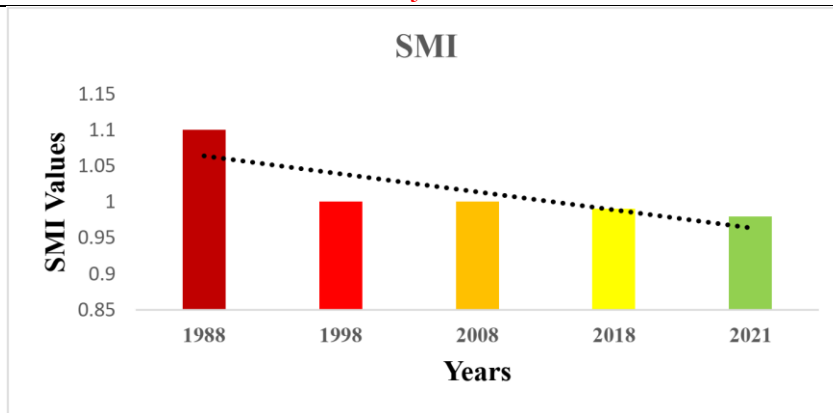


Figure 10: Graph showing the trendline of SMI values for the month of September in the years 1988, 1989, 2008, 2018, and 2021.

Relationship between LST and NDVI:

Figure 11 shows the comparative analysis between NDVI and LST. The trend line produced clarification, showing a strong inverse relationship between NDVI and LST. These results show that vegetation decreased due to the effects of LST. The -ve relationship between NDVI and LST predicts that the greater biomass of vegetation cover has lower LST. The LST and NDVI have a direct relation with the land cover changes. It also implies that images showing most reduced NDVI values have less vegetal spread due to the barren soil of the Thar desert, while the higher NDVI values have thick vegetal spread, and in this way, LST increase with the abundance in vegetal cover.

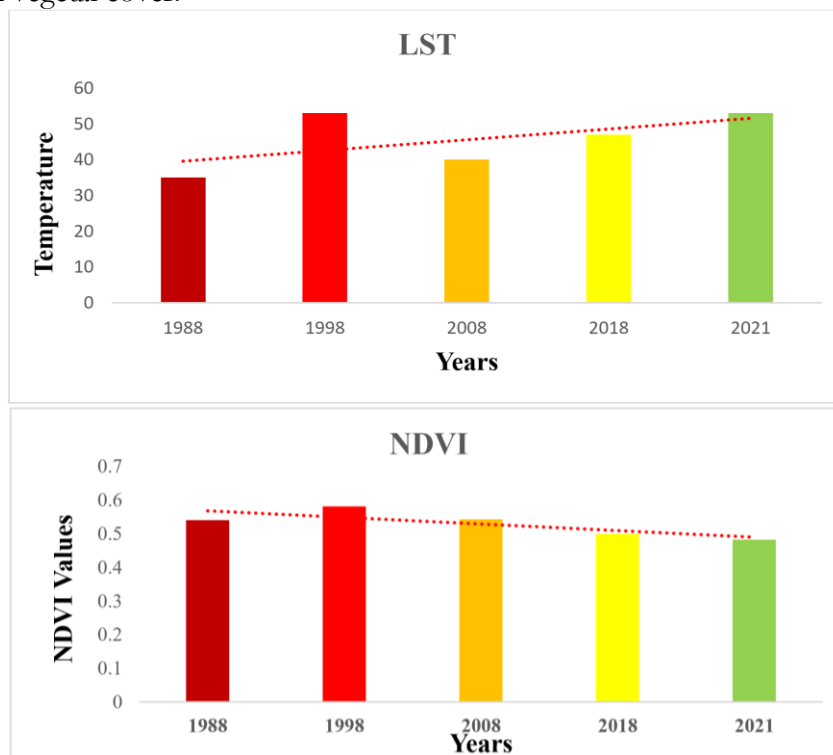


Figure 11: Graph showing the comparison between the trends of NDVI and LST values in the years 1988, 1989, 2008, 2018, and 2021.

There is a significant direct correlation between LST and NDVI, which makes it possible to forecast LST using direct regression if the NDVI values for the research area are provided. From this point forward, NDVI can be used to calculate the precise LST. The perception is that between 1988 and 2021, the NDVI values have declined as a result of expanding metropolitan areas and shrinking vegetated areas. Additionally, it distinguishes between places with high LST

being bare soil and regions with low temperature having more plant. The largest LST values show the littler NDVI and vice versa.

Conclusion:

Due to a lack of water resources, droughts are among the most frequent natural disasters that have a considerable negative influence on crop productivity. At four meteorological stations in Sindh, Pakistan, the RDI and SPI were estimated every three, six, and twelve months between 1981 and 2020. The results of the drought characterization show that throughout a 40-year period, the region experienced 4–6 years of moderate to severe drought. The three-month RDIs reveal that extreme, severe, and moderate drought episodes occurred every four to six years. Additionally, we talked about the accuracy and viability of the SPI and RDI in Sindh, Pakistan. Temperature deviations led to a decrease in precipitation, an increase in dry spells, and a general decrease in freshwater supplies for irrigation, all of which had a direct impact on the agricultural region and developments.

The SPI measures the departure from the long-term average of a normally distributed random variable. It is positive if the SPI is greater than the precipitation; otherwise, it is negative. A dry atmosphere is indicated by a low SPI. The results of the regression show that the SPI and RDI are closely related and may estimate the yearly RDI drought indicators even in the presence of data for the first three months of precipitation. The RDI time-series data's continuous decline indicates a rising pattern in drought severities. An increase in long-term drought severity could endanger the management of water resources in the studied regions because long-term droughts typically have an influence on water quality, especially ground water. In summary, the study demonstrates significantly low NDVI and SMI across the study period and high LST. The most important findings offer a vital basis for continuous checks of variations in land monitoring. They will be useful to decision-makers who want to improve plans for efficiently managing land resources. The results of this study will improve the ability of regional policymakers to create detailed regional and national land management strategies.

References:

- [1] J. M. Kirby et al., "The impact of climate change on regional water balances in Bangladesh," *Clim. Change*, vol. 135, no. 3–4, pp. 481–491, Apr. 2016, doi: 10.1007/S10584-016-1597-1/METRICS.
- [2] P. Kumar, S. F. Shah, M. A. Uqaili, L. Kumar, and R. F. Zafar, "Forecasting of Drought: A Case Study of Water-Stressed Region of Pakistan," *Atmos.* 2021, Vol. 12, Page 1248, vol. 12, no. 10, p. 1248, Sep. 2021, doi: 10.3390/ATMOS12101248.
- [3] G. Gebremeskel Haile et al., "Long-term spatiotemporal variation of drought patterns over the Greater Horn of Africa," *Sci. Total Environ.*, vol. 704, p. 135299, Feb. 2020, doi: 10.1016/J.SCITOTENV.2019.135299.
- [4] Y. Mao, Z. Wu, H. He, G. Lu, H. Xu, and Q. Lin, "Spatio-temporal analysis of drought in a typical plain region based on the soil moisture anomaly percentage index," *Sci. Total Environ.*, vol. 576, pp. 752–765, Jan. 2017, doi: 10.1016/J.SCITOTENV.2016.10.116.
- [5] M. Waseem, A. H. Jaffry, M. Azam, I. Ahmad, A. Abbas, and J. E. Lee, "Spatiotemporal Analysis of Drought and Agriculture Standardized Residual Yield Series Nexuses across Punjab, Pakistan," *Water* 2022, Vol. 14, Page 496, vol. 14, no. 3, p. 496, Feb. 2022, doi: 10.3390/W14030496.
- [6] T. Jiang, X. Su, V. P. Singh, and G. Zhang, "Spatio-temporal pattern of ecological droughts and their impacts on health of vegetation in Northwestern China," *J. Environ. Manage.*, vol. 305, p. 114356, Mar. 2022, doi: 10.1016/J.JENVMAN.2021.114356.
- [7] S. Adnan, K. Ullah, A. H. Khan, and S. Gao, "Meteorological impacts on evapotranspiration in different climatic zones of Pakistan," *J. Arid Land*, vol. 9, no. 6, pp. 938–952, Dec. 2017, doi: 10.1007/S40333-017-0107-2/METRICS.
- [8] U. Surendran, V. Kumar, S. Ramasubramoniam, and P. Raja, "Development of Drought

- Indices for Semi-Arid Region Using Drought Indices Calculator (DrinC) – A Case Study from Madurai District, a Semi-Arid Region in India,” *Water Resour. Manag.*, vol. 31, no. 11, pp. 3593–3605, Sep. 2017, doi: 10.1007/S11269-017-1687-5/METRICS.
- [9] S. Mukherjee, S. Aadhar, D. Stone, and V. Mishra, “Increase in extreme precipitation events under anthropogenic warming in India,” *Weather Clim. Extrem.*, vol. 20, pp. 45–53, Jun. 2018, doi: 10.1016/J.WACE.2018.03.005.
- [10] S. Hina, F. Saleem, A. Arshad, A. Hina, and I. Ullah, “Droughts over Pakistan: possible cycles, precursors and associated mechanisms,” *Geomatics, Nat. Hazards Risk*, vol. 12, no. 1, pp. 1638–1668, 2021, doi: 10.1080/19475705.2021.1938703.
- [11] C. Cammalleri, F. Micale, and J. Vogt, “A novel soil moisture-based drought severity index (DSI) combining water deficit magnitude and frequency,” *Hydrol. Process.*, vol. 30, no. 2, pp. 289–301, Jan. 2016, doi: 10.1002/HYP.10578.
- [12] N. Sánchez, Á. González-Zamora, M. Piles, and J. Martínez-Fernández, “A New Soil Moisture Agricultural Drought Index (SMADI) Integrating MODIS and SMOS Products: A Case of Study over the Iberian Peninsula,” *Remote Sens.* 2016, Vol. 8, Page 287, vol. 8, no. 4, p. 287, Mar. 2016, doi: 10.3390/RS8040287.
- [13] S. Fahad et al., “Crop production under drought and heat stress: Plant responses and management options,” *Front. Plant Sci.*, vol. 8, p. 265598, Jun. 2017, doi: 10.3389/FPLS.2017.01147/BIBTEX.
- [14] N. Salehnia, A. Alizadeh, H. Sanacinejad, M. Bannayan, A. Zarrin, and G. Hoogenboom, “Estimation of meteorological drought indices based on AgMERRA precipitation data and station-observed precipitation data,” *J. Arid Land*, vol. 9, no. 6, pp. 797–809, Dec. 2017, doi: 10.1007/S40333-017-0070-Y/METRICS.
- [15] Q. Liu et al., “Evaluating the performance of eight drought indices for capturing soil moisture dynamics in various vegetation regions over China,” *Sci. Total Environ.*, vol. 789, p. 147803, Oct. 2021, doi: 10.1016/J.SCITOTENV.2021.147803.
- [16] K. Xu, D. Yang, H. Yang, Z. Li, Y. Qin, and Y. Shen, “Spatio-temporal variation of drought in China during 1961–2012: A climatic perspective,” *J. Hydrol.*, vol. 526, pp. 253–264, Jul. 2015, doi: 10.1016/J.JHYDROL.2014.09.047.
- [17] D. Tigkas, H. Vangelis, and G. Tsakiris, “DrinC: a software for drought analysis based on drought indices,” *Earth Sci. Informatics*, vol. 8, no. 3, pp. 697–709, Sep. 2015, doi: 10.1007/S12145-014-0178-Y/METRICS.
- [18] D. Tigkas, H. Vangelis, and G. Tsakiris, “An enhanced effective reconnaissance drought index for the characterisation of agricultural drought,” *Environ. Process.*, vol. 4, no. 1, pp. S137–S148, Nov. 2017, doi: 10.1007/S40710-017-0219-X/METRICS.
- [19] A. Saha, M. Patil, V. C. Goyal, and D. S. Rathore, “Assessment and Impact of Soil Moisture Index in Agricultural Drought Estimation Using Remote Sensing and GIS Techniques,” *Proc.* 2019, Vol. 7, Page 2, vol. 7, no. 1, p. 2, Nov. 2018, doi: 10.3390/ECWS-3-05802.
- [20] W. Li et al., “Spatiotemporal characteristics of drought in a semi-arid grassland over the past 56 years based on the Standardized Precipitation Index,” *Meteorol. Atmos. Phys.*, vol. 133, no. 1, pp. 41–54, Feb. 2021, doi: 10.1007/S00703-020-00727-4/METRICS.
- [21] T. Iwata et al., “Preoperative serum value of sialyl Lewis X predicts pathological nodal extension and survival in patients with surgically treated small cell lung cancer,” *J. Surg. Oncol.*, vol. 105, no. 8, pp. 818–824, Jun. 2012, doi: 10.1002/JSO.23002.
- [22] D. Lang et al., “A Comparative Study of Potential Evapotranspiration Estimation by Eight Methods with FAO Penman–Monteith Method in Southwestern China,” *Water* 2017, Vol. 9, Page 734, vol. 9, no. 10, p. 734, Sep. 2017, doi: 10.3390/W9100734.
- [23] M. A. Asadi Zarch, B. Sivakumar, H. Malekinezhad, and A. Sharma, “Future aridity under conditions of global climate change,” *J. Hydrol.*, vol. 554, pp. 451–469, Nov. 2017,

doi: 10.1016/J.JHYDROL.2017.08.043.

- [24] S. Sruthi and M. A. M. Aslam, “Agricultural Drought Analysis Using the NDVI and Land Surface Temperature Data; a Case Study of Raichur District,” *Aquat. Procedia*, vol. 4, pp. 1258–1264, Jan. 2015, doi: 10.1016/J.AQPRO.2015.02.164.
- [25] A. R. Zarei, “Analysis of changes trend in spatial and temporal pattern of drought over south of Iran using standardized precipitation index (SPI),” *SN Appl. Sci.*, vol. 1, no. 5, pp. 1–14, May 2019, doi: 10.1007/S42452-019-0498-0/TABLES/6.
- [26] H. C. Kraemer and C. Blasey, “How Many Subjects?: Statistical Power Analysis in Research,” *How Many Subj. Stat. Power Anal. Res.*, Jan. 2016, doi: 10.4135/9781483398761.
- [27] M. Ben Abdelmalek and I. Nouiri, “Study of trends and mapping of drought events in Tunisia and their impacts on agricultural production,” *Sci. Total Environ.*, vol. 734, p. 139311, Sep. 2020, doi: 10.1016/J.SCITOTENV.2020.139311.
- [28] M. A. Amini, G. Torkan, S. Eslamian, M. J. Zareian, and J. F. Adamowski, “Correction to: Analysis of deterministic and geostatistical interpolation techniques for mapping meteorological variables at large watershed scales (*Acta Geophysica*, (2019), 67, 1, (191-203), 10.1007/s11600-018-0226-y),” *Acta Geophys.*, vol. 67, no. 1, p. 275, Feb. 2019, doi: 10.1007/S11600-018-0235-X/METRICS.



Copyright © by authors and 50Sea. This work is licensed under Creative Commons Attribution 4.0 International License.